OPEN

Oncogene (2016), 1–12

www.nature.com/onc

ORIGINAL ARTICLE

Cyclin G2 inhibits epithelial-to-mesenchymal transition by disrupting Wnt/β-catenin signaling

S Bernaudo[1], M Salem[1], X Qi[1], W Zhou[1], C Zhang[1], W Yang[1], D Rosman[1], Z Deng[2,5], G Ye[1], B Yang[2], B Vanderhyden[3], Z Wu[1,4] and C Peng[1]

Epithelial ovarian cancer (EOC) has the highest mortality rate among gynecological malignancies owing to poor screening methods, non-specific symptoms and limited knowledge of the cellular targets that contribute to the disease. Cyclin G2 is an unconventional cyclin that acts to oppose cell cycle progression. Dysregulation of the cyclin G2 gene (*CCNG2*) in a variety of human cancers has been reported; however, the role of cyclin G2 in tumorigenesis remains unclear. In this study, we investigated the function of cyclin G2 in EOC. *In vitro* and *in vivo* studies using several EOC-derived tumor cell lines revealed that cyclin G2 inhibited cell proliferation, migration, invasion and spheroid formation, as well as tumor formation and invasion. By interrogating cDNA microarray data sets, we found that *CCGN2* mRNA is reduced in several large cohorts of human ovarian carcinoma when compared with normal ovarian surface epithelium or borderline tumors of the ovary. Mechanistically, cyclin G2 was found to suppress epithelial-to-mesenchymal transition (EMT), as demonstrated by the differential regulation of various EMT genes, such as Snail, Slug, vimentin and E-cadherin. Moreover, cyclin G2 potently suppressed the Wnt/β-catenin signaling pathway by downregulating key Wnt components, namely LRP6, DVL2 and β-catenin, which could be linked to inhibition of EMT. Taken together, our novel findings demonstrate that cyclin G2 has potent tumor-suppressive effects in EOCs by inhibiting EMT through attenuating Wnt/β-catenin signaling.

Oncogene (2016) advance online publication, 15 February 2016; doi:10.1038/onc.2016.15

INTRODUCTION

Epithelial ovarian cancer (EOC) is the most lethal type of ovarian cancer and accounts for 90% of all reported cases.[1] The lack of effective early detection markers, coupled with the vague, non-specific symptoms of this malignancy, often results in the late diagnosis of the disease and makes EOC the most fatal of all gynecological malignancies and the fifth leading cause of cancer death in women.[2]

Cyclin G2 belongs to a group of unconventional cyclins that include cyclin G1 and cyclin I. Unlike typical cyclins, cyclin G2 expression is high in cells undergoing cell cycle arrest as well as in terminally differentiated cells.[3,4] Accumulating evidence suggests that cyclin G2 may have an important inhibitory role in cancer progression. First, growth-inhibitory signals enhance cyclin G2 levels, whereas many oncogenic signaling pathways inhibit its expression.[5,6] Second, we have previously reported that cyclin G2 inhibits EOC cell proliferation.[7] Similarly, overexpression of cyclin G2 reduces proliferation, colony formation and induces morphological changes in various cell types.[8–10] Finally, the expression level of cyclin G2 is negatively correlated with cancer progression and positively associated with patient survival.[10–12] For example, transforming growth factor-β and mutant p53 cooperate to promote breast cancer metastasis by opposing the activity of p63.[12] Furthermore, cyclin G2 has been identified as a key target of p63 and its level is associated with metastasis-free survival.[12] Despite its implication in human cancers, the exact functions and the underlying mechanism of cyclin G2 action in the development ovarian cancer and/or other malignancies remain unknown.

Epithelial-to-mesenchymal transition (EMT) is a process by which epithelial cells acquire motile and invasive properties, characteristic of mesenchymal-like cells.[13] EMT occurs naturally in development; however, it can be inappropriately exploited during carcinogenesis to augment oncogenic transformation of cancer cells, making them prone to migration and invasion. In the case of metastatic ovarian cancer, cells or cell spheroids are exfoliated from the primary site and enter the peritoneal cavity where they spread via malignant ascites.[14] Ovarian spheroids often maintain their mesenchymal characteristics, with reduced E-cadherin expression, and a more aggressive phenotype.[15]

Various signaling cascades are known to contribute to the onset of EMT, including the Wnt pathway.[16] In the canonical Wnt pathway, absence of Wnt ligands promotes the formation of the β-catenin destruction complex, leading to the phosphorylation and degradation of β-catenin by the proteasome. When the pathway is stimulated, the Wnt receptors, frizzled and low-density lipoprotein receptor-related protein (LRP) 5/6 associate with Dishevelled (DVL) to facilitate the interaction of the destruction complex to the cytoplasmic tail of LRP, inhibiting its action on β-catenin. In this respect, free β-catenin accumulates in the cytoplasm and translocates to the nucleus where it activates the transcription of its target genes.[17] Wnt/β-catenin signaling is implicated in the regulation of both carcinogenesis and EMT.[17,18] In ovarian cancer cells, decreased β-catenin signaling reverses EMT and suppresses malignancy.[19]

We have previously reported that cyclin G2 inhibits EOC proliferation.[7,20] To further understand the role of cyclin G2 in

[1]Department of Biology, York University, Toronto, Ontario, Canada; [2]Sunnybrook Research Institute, Sunnybrook Health Sciences Centre, Toronto, Ontario, Canada; [3]Department of Cellular and Molecular Medicine, University of Ottawa, Ottawa, Ontario, Canada and [4]Division of Life Science, Hong Kong University of Science and Technology, Hong Kong, China. Correspondence: Professor C Peng, Department of Biology, York University, 4700 Keele Street, Toronto, Ontario M3J 1P3, Canada.
E-mail: cpeng@yorku.ca
[5]Current address: People's Hospital of Jiangsu University, Zhenjiang, Jiangsu, China.
Received 9 August 2015; revised 14 December 2015; accepted 5 January 2016

ovarian cancer development, we examined the function of cyclin G2 in EOC cells and investigated its mechanism of action. We demonstrate that cyclin G2 inhibits EOC cell proliferation, migration and invasion by inhibiting Wnt/β-catenin activity and EMT.

RESULTS

Cyclin G2 suppresses cell proliferation, migration, invasion and spheroid formation in EOCs

As cyclin G2 was shown to be dysregulated in a variety of human cancers, we compared cyclin G2 mRNA levels in several EOC cell lines to those in normal ovary and Fallopian tube and found significantly lower levels of cyclin G2 in EOC cells than in normal tissues (Supplementary Figure S1A). Because of the highly unstable nature of cyclin G2,[7] we generated various cell lines that stably express cyclin G2 and confirmed the expression of exogenous cyclin G2 by western blotting, immunofluorescence and quantitative real-time PCR (qPCR) analysis (Supplementary Figures S1B–D). We found that overexpression of cyclin G2 significantly reduced proliferation in multiple EOC cell lines (Figures 1a and b and Supplementary Figure S2A), whereas the apoptotic markers, cleaved-PARP and -caspase-3 remained similar between cyclin G2 and control cells (Supplementary Figure S2B). Furthermore, cyclin G2 strongly reduced the clonogenicity of EOC cells resulting in smaller and fewer colonies (Figure 1c and Supplementary Figure S2C).

Next we investigated the role of cyclin G2 in migration and invasion. Using a scratch-wound assay, we found that cyclin G2 strongly attenuated cell migration (Figure 2a and Supplementary Figure S3A). In transwell invasion assays, the cells stably transfected with cyclin G2 displayed decreased invasive capacity when compared with the empty vector control (Figure 2b and Supplementary Figure S3B). To further confirm the anti-migratory and anti-invasive effects of cyclin G2, we performed transwell migration and invasion assays with cells pretreated with the proliferation inhibitor, mitomycin C. Cyclin G2 significantly reduced the number of cells migrated or invaded through the transwell insert (Figure 2c). The ability of EOC cells to form tight spheroids is characteristic of more aggressive tumor cells.[21] Using a three-dimension cell culture that better represents the *in vivo* arrangement of metastasizing ovarian cancer cells, we found that the SKOV3.ip1 cells overexpressing cyclin G2 formed much looser spheroids than the control cells, which formed well-defined and compact aggregates (Figure 2d). Similar results were obtained from HEY and ES-2 cells (Supplementary Figure S4A). When these spheroids were embedded into collagen I, cell migration and invasion were strongly inhibited as demonstrated by reduced cellular penetration into the surrounding matrix (Figure 2d and Supplementary Figure S4B).

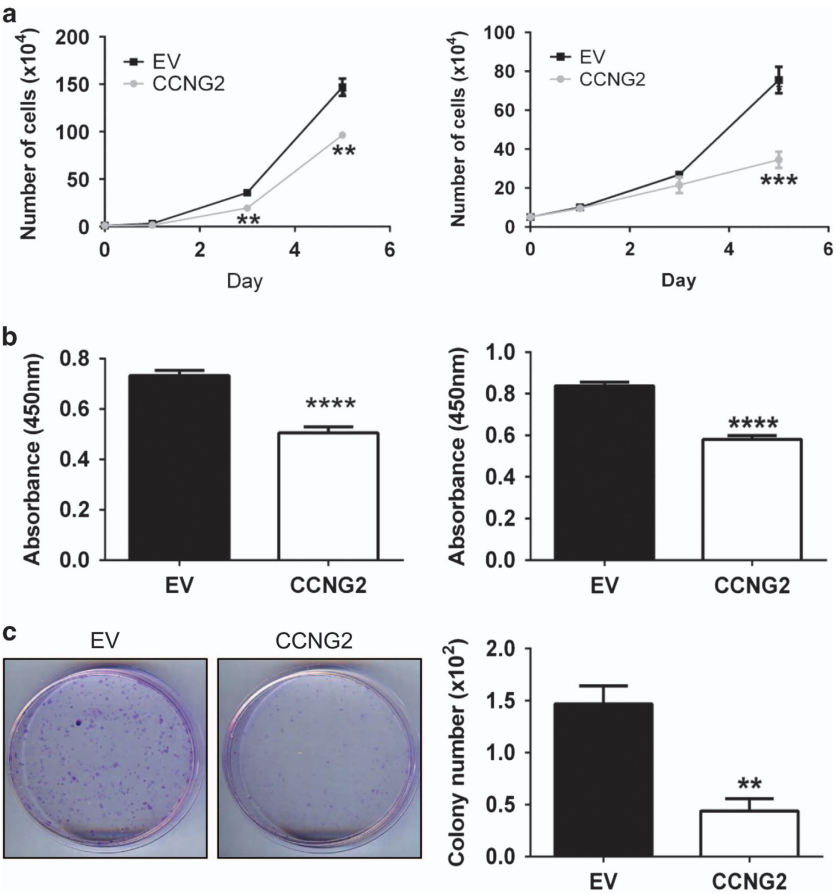

Figure 1. Cyclin G2 suppresses ovarian cancer cell proliferation. (**a**) Trypan blue exclusion assays. SKOV3.ip1 (left panel) and ES-2 (right panel) cells stably expressing cyclin G2 (CCNG2) or its control vector (EV) were plated at equal density and cultured for 1, 3 and 5 days ($n = 3$). (**b**) BrdU proliferation assay of SKOV3.ip1 (left panel) and ES-2 (right panel) cells stably expressing CCNG2 or its control vector (EV). Cells were plated in a 96-well plate and incubated for 72 h prior to BrdU incorporation and detection ($n = 10$). (**c**) Clonogenic assay. ES-2 stable cells were plated at low density and cultured for 12 days. Representative pictures (left panel) and a summary graph (right panel) are shown ($n = 3$). $^{**}P < 0.01$; $^{***}P < 0.001$; $^{****}P < 0.0001$ vs EV.

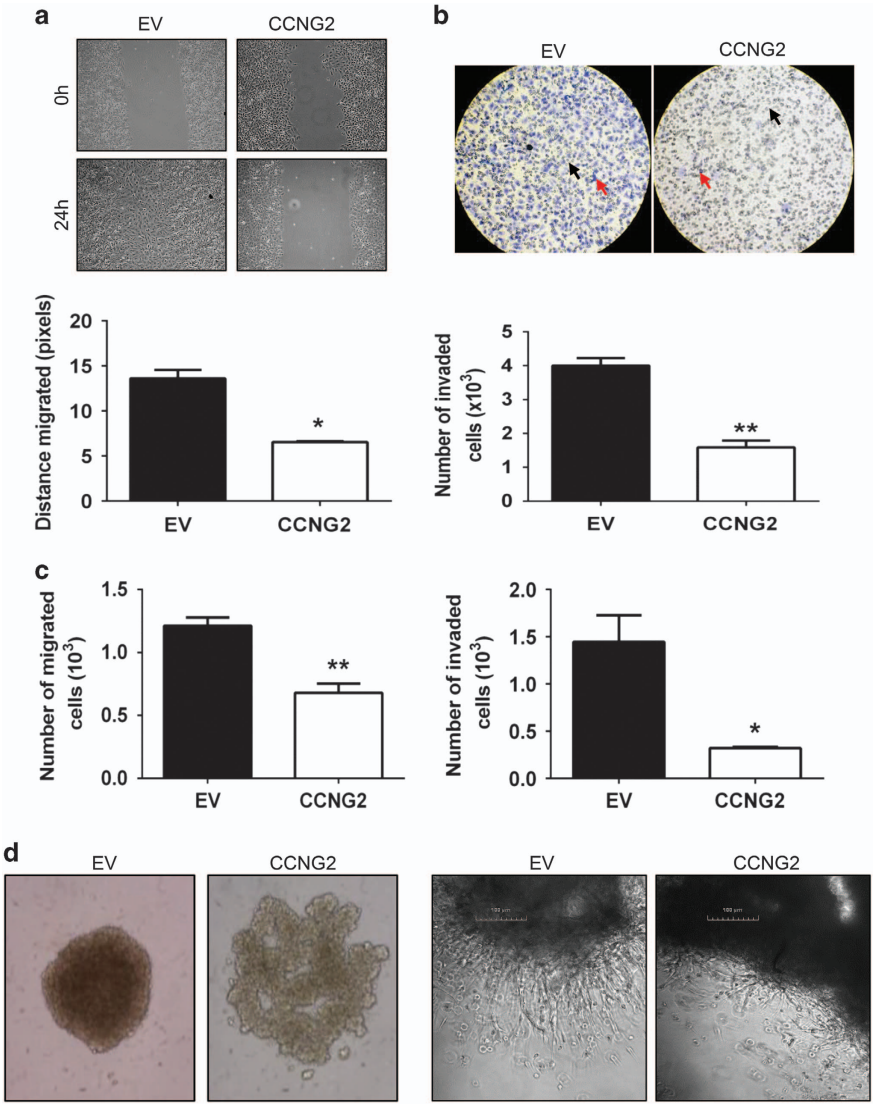

Figure 2. Cyclin G2 (CCNG2) suppresses ovarian cancer cell migration, invasion and spheroid formation. (**a**) Wound-healing assays using SKOV3.ip1 stable cells. Pictures were taken right after the wound was created (0 h) and 24 h later. Representative pictures (top panel) and a summary graph (bottom panel) are presented ($n = 3$). (**b**) Matrigel-coated transwell-invasion assays of SKOV3.ip1 stable cells. Red arrows indicate invaded cells while black arrows denote transwell pores ($n = 3$). (**c**) SKOV3.ip1 stable cells were treated with mitomycin C for 2 h prior to transwell migration (left panel) and invasion (right panel). Representative graphs are shown ($n = 3$). (**d**) Spheroid formation and invasion assays. Hanging drop cultures were performed using SKOV3.ip1 stable cells. Spheroids were observed and photographed 4 days after plating (left panel) and then embedded into collagen I. Degree of cell invasion was observed by cellular penetration into the surrounding matrix after 3 days (right panel). *$P < 0.05$; **$P < 0.01$ vs empty vector control (EV).

Cyclin G2 inhibits tumor development *in vivo*

To study the *in vivo* effect of cyclin G2 on tumor progression, SKOV3.ip1 stable cells were injected subcutaneously into nude mice. Cyclin G2 cells formed small tumors that did not grow significantly over the course of the experiment, whereas mice injected with control cells produced tumors that grew much larger (Figure 3a). Similarly, in cyclin G2-overexpressing ES-2 cells, tumor formation was strongly inhibited (Supplementary Figure S5). Immunohistochemistry revealed that, unlike the tumors formed by control cells, tumors produced from cyclin G2-overexpressing cells failed to invade the surrounding muscle tissue layer (Figure 3b). Furthermore, intraperitoneal injection with ES-2 cells stably transfected with cyclin G2 had decreased accumulation of ascites fluid, body weight and distension of the abdomen when compared with the mice inoculated with control cells (Figure 3c).

Cyclin G2 is downregulated in EOC tumors

To determine whether cyclin G2 is dysregulated during EOC development, we interrogated ovarian cancer microarray data sets on Oncomine and found lower cyclin G2 mRNA levels in ovarian carcinoma when compared with normal ovarian surface epithelium or borderline tumors of the ovary (Figures 3d–f and Supplementary Figure S6A). Consistent with these results, qPCR of human ovarian tumor samples revealed lower cyclin G2 mRNA levels in high-grade carcinomas compared with the low malignant potential tumors in all histological subtypes of ovarian cancer analyzed (Supplementary Figure S6B). Similarly, data retrieved from the Hendrix Ovarian data set[22] on Oncomine showed consistently higher levels of cyclin G2 in normal ovary compared with the clear cell, mucinous, endometrioid and serous subtypes of ovarian cancers (Supplementary Figure S6C).

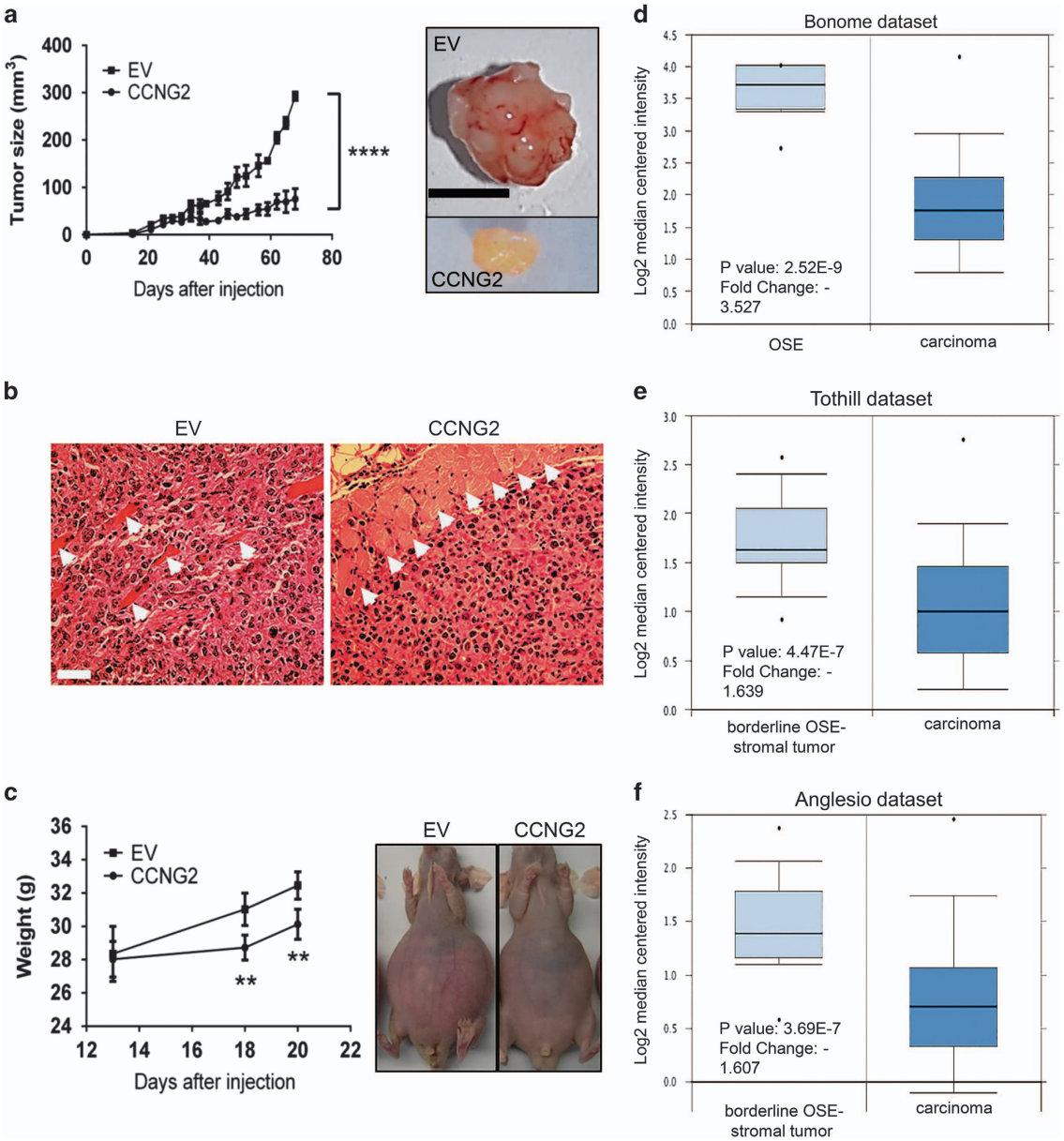

Figure 3. Cyclin G2 (CCNG2) inhibits *in vivo* tumor formation and its expression is reduced in human ovarian carcinoma. (**a**) SKOV3.ip1 stable cells expressing control vector (EV) or CCNG2 were injected subcutaneously into nude mice. Tumor sizes were measured after sizeable tumors began to form (day 15), and mice were killed on day 68 ($n=4$ for EV and $n=5$ for CCNG2). (**b**) Hematoxylin and eosin staining of tumor sections showing invasion of tumor cells into surrounding smooth muscle (arrow heads). Scale bar = 50 mm ($n=3$). (**c**) ES-2 stable cells were injected intraperitoneally into nude mice ($n=3$). Mice were weighed on days 13, 18 and before killing on day 20 ($n=3$). Representative pictures of mice inoculated with EV or CCNG2-overexpressing cells. $^{**}P<0.01$; $^{****}P<0.0001$ vs EV. (**d**–**f**) Interrogation of ovarian cancer microarray data sets using Oncomine (www.oncomine.org). (**d**) Lower *CCNG2* levels were found in ovarian carcinoma ($n=185$) when compared with normal ovarian surface epithelium (OSE, $n=10$) in the Bonome data set.[46] (**e**) Significantly lower *CCNG2* expression is found in ovarian carcinoma ($n=171$) compared with borderline OSE and stromal tumors ($n=18$) in the Tothill data set.[47] (**f**) Anglesio data set comparing *CCNG2* mRNA levels in borderline tumors ($n=30$) and ovarian carcinoma ($n=44$).[44]

Cyclin G2 inhibits EMT

EMT has a critical role in tumor development by reverting epithelial cells to a more mesenchymal state.[13] In cyclin G2-overexpressing cells, we observed morphological changes representative of epithelial cells. Although control cells displayed spindle-shaped morphology, cyclin G2-overexpressing cells were rounded and showed greater cell-to-cell contacts (Figure 4a). To test the hypothesis that cyclin G2 may regulate EMT, we examined a panel of EMT marker genes, including *CDH1* (E-cadherin), *SNAI1* (Snail), *SNAI2* (Slug), *ZEB1*, *ZEB2*, *CDH2* (N-Cadherin) and *VIM* (vimentin), and found that cyclin G2 increased the mRNA level of epithelial marker *CDH1* but decreased the mesenchymal markers (Figure 4b and Supplementary Figure S7A). Moreover, the high-mobility group AT-hook 2, which is a marker of poorly differentiated cancers,[23] was shown to be decreased in cyclin G2-overexpressing cells (Figure 4b). Similarly, the protein level of E-cadherin was upregulated in cyclin G2 cells, accompanied by a decrease in vimentin levels (Figure 4c and Supplementary Figure S7B). Finally, in tumors formed from cyclin G2-overexpressing cells, E-cadherin levels were strongly enhanced when compared with the control (Figure 4d).

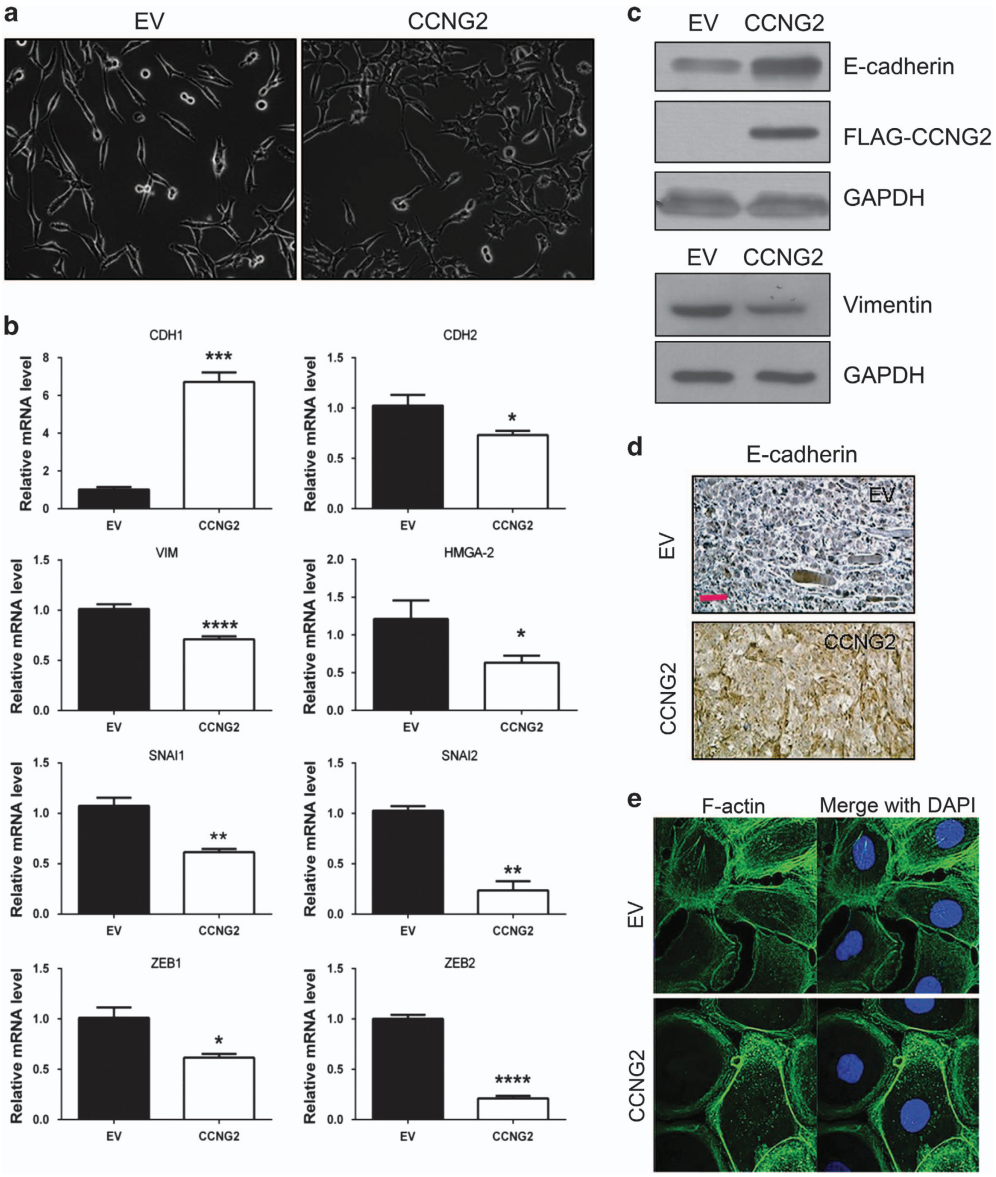

Figure 4. Cyclin G2 (CCNG2) inhibits EMT in EOC cells. (**a**) Morphological changes in cells stably transfected with CCNG2. CCNG2 overexpression resulted in greater cell–cell contacts when compared with cells transfected with empty vector (EV). (**b**) mRNA levels of several EMT makers in EV and CCNG2-overexpressing SKOV3.ip1 cells ($n = 3$). *$P < 0.05$; **$P < 0.01$; ***$P < 0.001$; ****$P < 0.0001$ vs EV. (**c**) Protein levels of the EMT markers, E-cadherin and vimentin in SKOV3.ip1 stable cells assessed by western blotting. (**d**) Immunohistochemistry of tumor sections obtained from mice subcutaneously injected with EV or CCNG2 stable cells, using an anti-E-cadherin antibody. Scale bar = 50 mm. (**e**) Immunofluorescent staining of F-actin using phalloidin–fluorescein isothiocyanate in SKOV3.ip1 stable cells.

To further investigate the effect of cyclin G2 on EMT, we examined the organization of actin filaments. Using immunofluorescence, we observed a more bundled and circumferential arrangement of the F-actin in the cyclin G2-overexpressing cells, while the empty vector control group exhibited a more complex array of F-actin, which denotes morphological changes associated with mesenchymal-type cells (Figure 4e).

Silencing of cyclin G2 enhances cell migration and augments EMT markers

As SKOV3.ip1 cells expressed the highest *CCNG2* mRNA of the EOC cell lines tested, we determined whether silencing of cyclin G2 in these cells would affect the expression of EMT marker genes and cell migration. As shown in Figure 5, knockdown of cyclin G2 (Figure 5a) resulted in increased cell migration (Figure 5b). In addition, *CDH1* mRNA was decreased, whereas mesenchymal markers *VIM*, *SNAI1*, *SNAI2* and *ZEB2* were all increased when cyclin G2 expression was silenced (Figure 5c).

Cyclin G2 attenuates Wnt/β-catenin signaling

E-cadherin has been reported to inhibit EOC growth by forming a complex with β-catenin at the adherens junction, sequestering it at the membrane and inhibiting the activation of its target genes.[24] Therefore, we tested whether cyclin G2 inhibits EOC by suppressing β-catenin signaling. Immunofluorescence revealed that β-catenin was diffusely organized with a greater proportion found in the nucleus. However, in cyclin G2-overexpressing cells, nuclear β-catenin was reduced while more β-catenin was

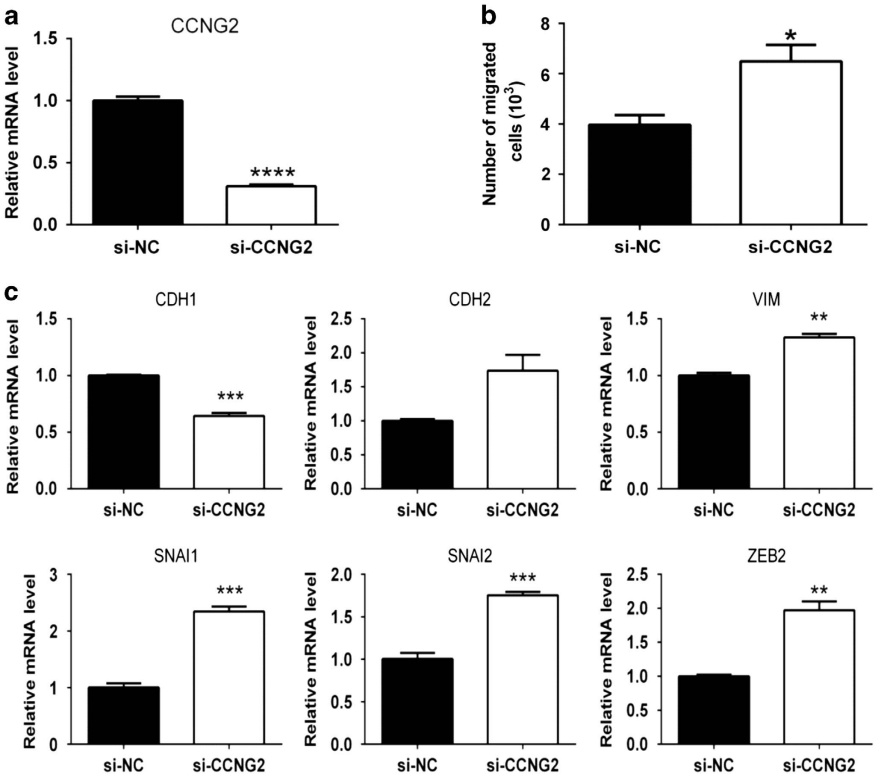

Figure 5. Silencing of cyclin G2 in SKOV3.ip1 enhances cell migration and augments EMT markers. (**a**) Cyclin G2 (*CCNG2*) mRNA levels in cells transfected with siRNA targeting *CCNG2* (si-CCNG2) or its negative control (si-NC). (**b**) Knockdown of *CCNG2* by siRNA increased cell migration in transwell migration assay. (**c**) mRNA levels of several EMT makers in negative control and si-CCNG2 transfected cells ($n = 3$). $^*P < 0.05$; $^{**}P < 0.01$; $^{***}P < 0.001$; $^{****}P < 0.0001$ vs si-NC.

accumulated at the cell periphery (Figure 6a). Cell fractionation revealed that cyclin G2 decreased β-catenin levels in both the cytoplasmic and nuclear fractions (Figure 6b). In addition, total β-catenin levels were found to be lower in the cyclin G2-overexpressing cells compared with the control, whereas the phosphorylated form of β-catenin at Ser33, Ser37 and Thr41 was enhanced (Figure 6c and Supplementary Figure S7C). Furthermore, a significant decrease in the expression of the β-catenin target mRNAs, *AXIN2*, *LEF1* and *TCF1*, was observed in the cyclin G2 cells compared with the control cells (Figure 6d). Finally, cyclin G2 significantly suppressed the transcriptional activity of β-catenin, as measured by the TOPFlash luciferase reporter assays (Figure 6e and Supplementary Figure S7D).

In the canonical Wnt/β-catenin pathway, β-catenin is protected from degradation when Wnt ligands bind to their receptors. To explore the mechanisms by which cyclin G2 decreased β-catenin levels and activity, we examined the protein level of several key molecules involved in Wnt signaling and found that DVL2 and LRP6 were inhibited by cyclin G2 (Figure 6f). However, there was no difference in *DVL2* and *LRP6* mRNA levels (Supplementary Figure S7E). To further confirm the regulation of LRP6, DVL2 and β-catenin by cyclin G2, SKOV3.ip1 cells were transiently transfected with FLAG-tagged cyclin G2, and protein samples were collected before transfection or at various time points thereafter. At 5 h posttransfection, cyclin G2 expression was detected along with a decrease in LRP6 levels while a subsequent and sustained decrease in DVL2 and β-catenin was observed 8 h after transfection (Figure 6g).

Cyclin G2 functions are attenuated by constitutively active β-catenin or silencing of E-cadherin

To determine whether inhibition of β-catenin is critical for the observed effects of cyclin G2, we tested whether constitutive activation of β-catenin could reverse the action of cyclin G2. The mutant β-catenin (S33Y) is resistant to phosphorylation and is not recognized by the proteasome for degradation. Transfection of the S33Y-β-catenin mutant (Figure 7a) reversed the effect of cyclin G2 on E-cadherin and vimentin expression (Figure 7b), as well as cell proliferation and migration (Figure 7c).

β-catenin can indirectly decrease E-cadherin expression via upregulation of its transcriptional repressors.[25,26] Therefore, we examined whether silencing of E-cadherin would reverse the effects of cyclin G2. Knockdown of E-cadherin using siRNA (Supplementary Figure S8A) reversed the suppressive effects of cyclin G2 on proliferation, migration and invasion (Figure 7d and Supplementary Figures S8B and C). In the 3D hanging drop culture, knockdown of E-cadherin in the cyclin G2 cells rescued the well-defined and compact formation of spheroids (Supplementary Figure S8D). These results suggest that attenuation of β-catenin signaling and induction of E-cadherin are important mechanisms by which cyclin G2 exerts its antitumor effects.

DISCUSSION

The present study was carried out to investigate if and how cyclin G2 is involved in ovarian cancer progression. Multiple lines of evidence often implicate cyclin G2 as part of signaling cascades that inhibit tumor progression. However, its role in ovarian cancer and its molecular mechanisms have yet to be elucidated. Our study demonstrates that cyclin G2 exerts antitumor effects in ovarian cancer cells by inhibiting EMT and attenuating Wnt/β-catenin signaling.

Accumulating evidence suggests that cyclin G2 expression is negatively correlated with cancer progression and positively associated with patient survival. In various human cancers, cyclin

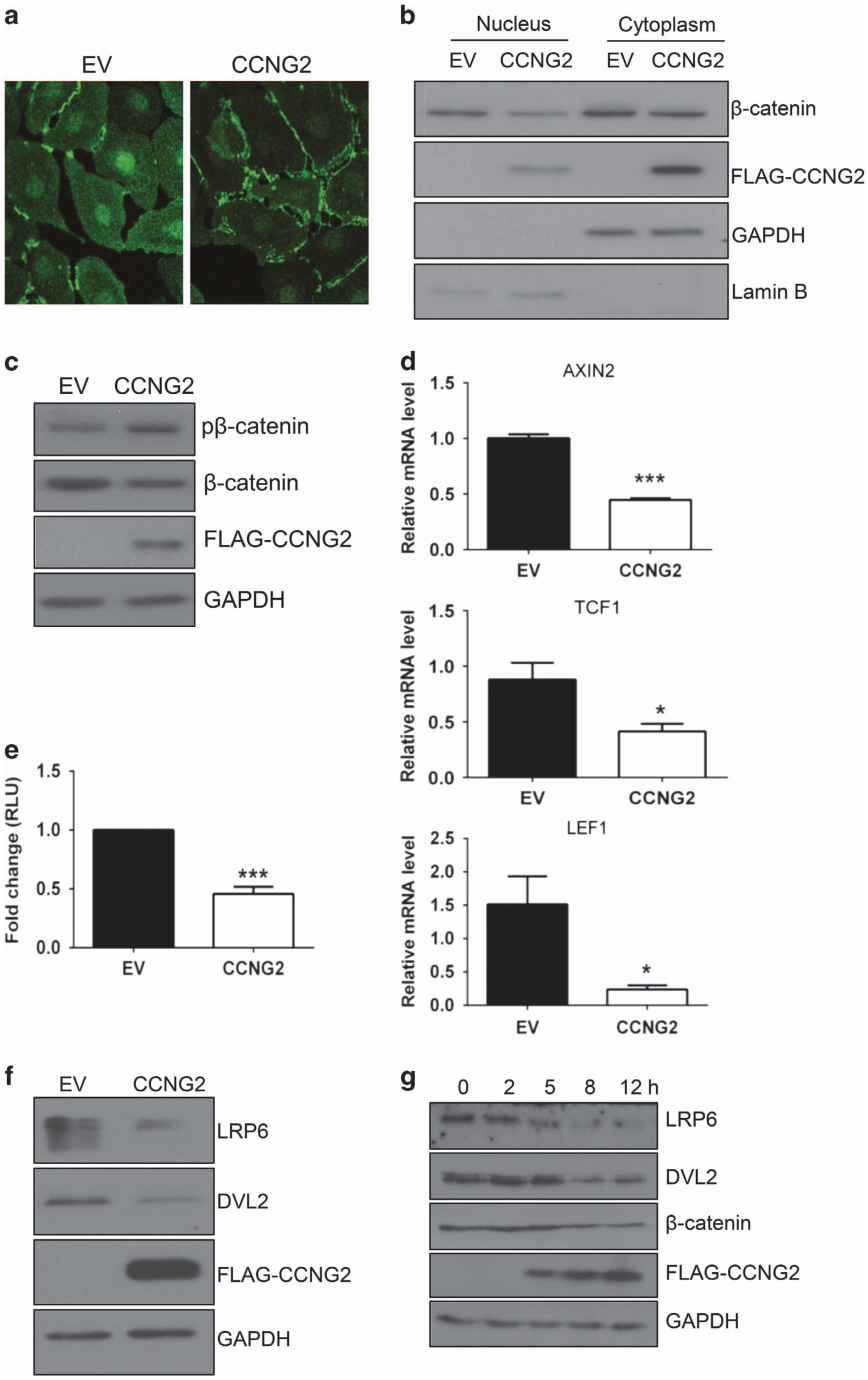

Figure 6. Cyclin G2 (CCNG2) attenuates Wnt/β-catenin signaling. (**a**) Immunofluorescence staining of β-catenin in SKOV3.ip1 stable cells. CCNG2 overexpression directed β-catenin away from the nucleus to the membrane, while the empty vector (EV) cells showed a higher nuclear stain. (**b**) Cyclin G2 reduced cytosolic and nuclear β-catenin levels. Cells lysates were prepared from cytosolic and nuclear fractions. β-catenin, GAPDH (cytosolic control) and Lamin B (nuclear control) were analyzed by western blotting. (**c**) Western blotting analysis of phospho and total β-catenin in control and CCNG2 stable cells. (**d**) Relative transcript levels of β-catenin target genes, *AXIN2*, *TCF1* and *LEF1*, as measured by qPCR ($n = 3$). (**e**) TOPFlash luciferase reporter assay for β-catenin transcriptional activity ($n = 3$). (**f**) Western blotting analysis showing that LRP6 and DVL2 levels were reduced in cells stably transfected with CCNG2. (**g**) Western blotting analysis of cells transiently transfected with the FLAG-CCNG2 plasmid. Protein samples were prepared at the time points indicated immediately following transfection. $^{*}P < 0.05$; $^{***}P < 0.001$ vs EV.

G2 is significantly lost as cells move through a step-wise cancer progression model,[10,27] and its expression has been shown to be inversely correlated with more advanced stages of disease.[11,28] However, little is known about the expression level and biological function of cyclin G2 in ovarian cancer. Interrogation of several large cohorts of datasets found on Oncomine and analysis of human clinical samples revealed a lower cyclin G2 mRNA level in advanced ovarian carcinoma samples, suggesting that the loss of cyclin G2 may contribute to EOC development. Collectively, these findings, coupled with a poor understanding of cyclin G2 function, warrant the full investigation of cyclin G2 in both normal and malignant cells.

Previous studies have shown that cyclin G2 can suppress proliferation in a variety of cells.[4,7,8,10,29] In this study, we used

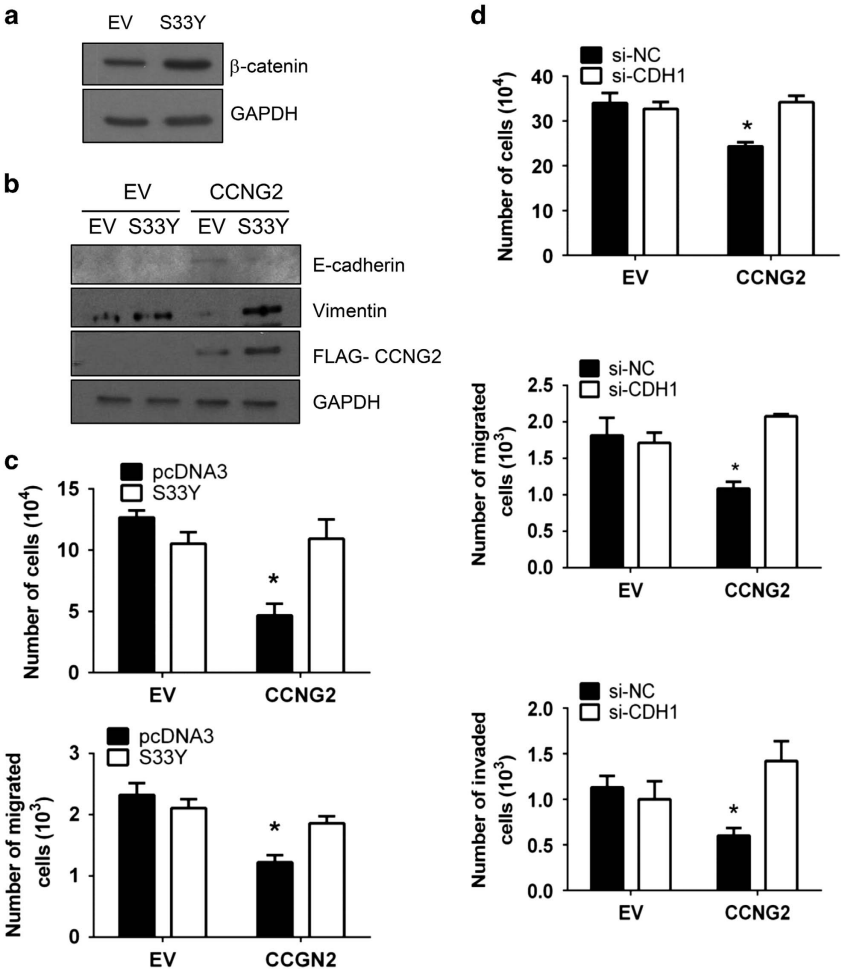

Figure 7. β-Catenin and E-cadherin are involved in the action of cyclin G2 (CCNG2). (**a**) Transient transfection of constitutively active β-catenin (S33Y). (**b**) β-Catenin S33Y mutant rescued the expression of vimentin and decreased E-cadherin protein levels in SKOV3.ip1 stably transfected with CCNG2. (**c**) β-Catenin S33Y mutant reversed the effect of CCNG2 on cell proliferation assay (top panel) and migration assay (bottom panel). Control (EV) and CCNG2-stable cells were transiently transfected with control vector or β-catenin-S33Y, and trypan blue exclusion or transwell migration assays were performed at 48 h after transfection. (**d**) Silencing of E-cadherin attenuated the effects of CCNG2. EV or CCNG2 cells were transfected with E-cadherin siRNA (si-CDH1) or its scrambled control (si-NC). Cell proliferation (top panel), migration (middle panel) and invasion (bottom panel) were measured ($n = 3$). *$P < 0.05$ vs all other groups.

various approaches to comprehensively analyze the role of cyclin G2 and provided strong evidence that cyclin G2 exerts antitumor effects in EOC cells. Specifically, cyclin G2 inhibits cell proliferation, migration and invasion, which can account for the observed decreased tumor burden *in vivo*. Likewise, silencing of cyclin G2 increased cell migration. These findings support the notion that loss of cyclin G2 contributes to the development of EOC.

The present work has uncovered molecular mechanisms by which cyclin G2 exerts antitumor effects. Many studies have suggested that EMT has a key role in EOC metastasis. For example, EMT is thought to regulate mesothelial cell clearance and drive early dissemination of EOC cells into the peritoneal cavity.[30] In addition, metastasizing ovarian cancer cells can be clearly distinguished from the primary tumor sample of the same patient by an expression signature of genes associated with EMT.[31] Furthermore, various genes that induce EMT are also associated with increased tumor aggressiveness, stemness and chemoresistance.[32–34] We observed that cyclin G2 upregulated the expression of E-cadherin but suppressed the expression of several mesenchymal markers. Phenotypically, cyclin G2-overexpressing cells exhibited epithelial characteristics, typical of less metastatic tumor cells.[35] Finally, siRNA-mediated knockdown of E-cadherin attenuated the antitumor effects of cyclin G2. These findings strongly suggest that inhibition of EMT is a major mechanism by which cyclin G2 inhibits ovarian cancer development.

Canonical Wnt/β-catenin signaling is important to the induction of EMT.[36,37] Dysregulated signaling of the Wnt/β-catenin pathway has been shown to increase proliferation and malignancy of various human cancers, including ovarian.[16] We observed that cyclin G2 enhanced membrane-associated β-catenin, whereas decreased nuclear β-catenin and suppressed β-catenin transcriptional activity. It is proposed that Wnt ligand binding to its receptor promotes the interaction of DVL with the Wnt-co-receptors to facilitate the interaction between LRP and the β-catenin destruction machinery. Sequestering of the destruction complex allows β-catenin to enter the nucleus and regulate transcription.[17] Interestingly, we observed downregulation of DVL2 and LRP6 by cyclin G2. Therefore, it is possible that cyclin G2 decreases the level of Wnt mediators, leading to reduced Wnt activity and destruction of β-catenin.

Several lines of evidence suggest that attenuation of the Wnt/β-catenin pathway is responsible, at least in part, for the inhibition of EMT by cyclin G2. First, stable or transient transfection of cyclin G2 decreased Wnt/β-catenin signaling. Second, constitutively active

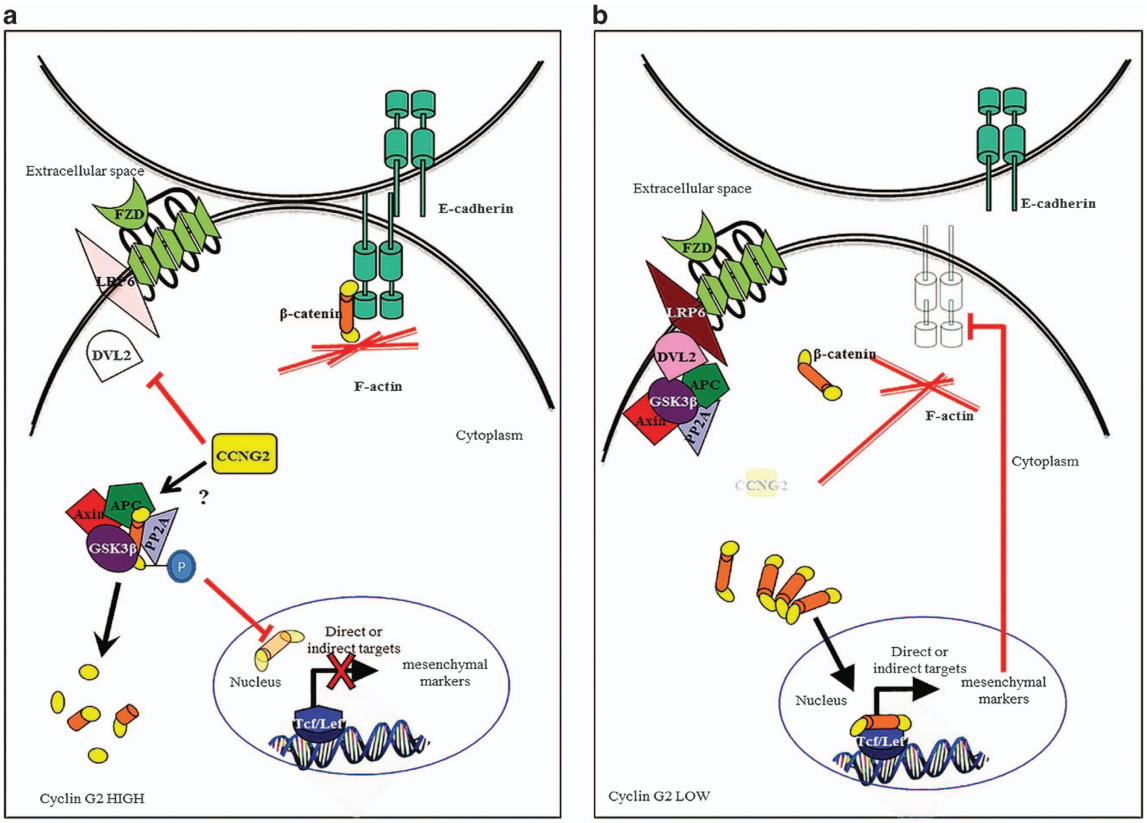

Figure 8. Proposed mechanism of cyclin G2 (CCNG2) action in ovarian cancer cells. (**a**) CCNG2 inhibits Wnt signaling by suppressing LRP6 and DVL2 expression, resulting in the activation of the β-catenin destruction complex and the degradation of cytosolic β-catenin. Inhibition of β-catenin suppresses TCF/LEF signaling and prevents the induction of its downstream target genes. Subsequent inhibition of pro-EMT transcription factors promotes the expression of E-cadherin, which in turn further sequesters β-catenin at the membrane. In addition, E-cadherin and β-catenin form a complex with F-actin, which modulates cytoskeleton dynamics and decreases the migratory capacity of cancer cells. (**b**) Low CCNG2 expression allows for the accumulation of β-catenin in the cytoplasm. Free β-catenin can translocate to the nucleus and stimulate the transcription of genes that contribute to EMT in ovarian cancer cells.

β-catenin reversed the effect of cyclin G2 on E-cadherin and vimentin expression. Furthermore, previous reports have shown that the inhibition of Wnt signaling in ovarian cancer cells diminished the capacity of cells to adhere and migrate, which was attributed to the inhibition of EMT.[38]

Although data presented here clearly defines the inhibitory role of cyclin G2 on Wnt/β-catenin signaling, how cyclin G2 exerts its effects on LRP6, DVL2 and β-catenin remains to be investigated in the future. Cyclin G2 has been reported to regulate gene transcription in cooperation with other transcription factors, such as peroxisome proliferator-activated receptor-γ.[39] In this study, we also observed that cyclin G2 is present in both the cytoplasm and nucleus. However, we did not detect changes in *DVL2* or *LRP6* mRNA levels. Furthermore, we found that decrease in LRP6 and DVL2 occurred rapidly following cyclin G2 transfection. These findings suggest that cyclin G2 inhibits LRP6 and DVL2 mainly by enhancing their degradation. Cyclin G2 has been recently reported to promote autophagy in chronic myeloid leukemia cells,[40] and autophagy has been shown to inhibit Wnt signaling by induction of DVL2 degradation.[41] In addition, as we have found that cyclin G2 caused an upregulation of the phosphorylated form of β-catenin, it is possible that it may also regulate the activity and/or stability of the β-catenin destruction complex. Indeed, cyclin G2 can form a complex with protein phosphatase 2A (PP2A),[8] and the association of PP2A in the β-catenin destruction complex has been described.[42] Therefore, cyclin G2 may act to correctly distribute one or more of these proteins to the destruction complex for efficient degradation of β-catenin. Future studies will aim to elucidate the mechanisms by which cyclin G2 regulates the canonical Wnt pathway.

We propose that cyclin G2 suppresses malignancy by maintaining an epithelial phenotype through attenuation of β-catenin signaling in ovarian cancer cells. Specifically, cyclin G2 downregulates critical components of the Wnt pathway, namely, LRP6, DVL2 and β-catenin, resulting in inhibition of mesenchymal genes and upregulation of E-cadherin. In addition, E-cadherin sequesters β-catenin at the membrane and forms a complex with F-actin, which modulates cytoskeleton dynamics and decreases the migratory capacity of cancer cells (Figure 8a). Low cyclin G2 expression, as observed in cancer cells, will contribute to higher activity of Wnt/β-catenin and confer ovarian cancer cells with more aggressive characteristics (Figure 8b). We suggest that the loss of cyclin G2 may define a critical turning point in oncogenesis that promotes EMT and cancer cell dissemination, leading to metastasis.

Taken together, our study conceptually advances the current understanding of the molecular mechanisms by which cyclin G2 functions, especially within the context of Wnt signaling, and highlights the importance of cyclin G2 in inhibiting ovarian cancer progression. Our findings further support the Wnt/β-catenin pathway as a potential therapeutic target for ovarian cancer. Future studies will investigate how cyclin G2 is regulated and explore the possibility of suppressing the pathways that inhibit cyclin G2 or promote β-catenin signaling as targeted therapies for ovarian cancer.

MATERIALS AND METHODS

Cell lines and cell culture

Four different EOC cell lines were used in this study. ES-2, SKOV3 (both purchased from American Type Culture Collection, Manassas, VA, USA) and SKOV3.ip1 (kindly provided by Dr Mien-Chie Hung, MD Anderson Cancer Center, Houston, TX, USA) were maintained in McCoy's (Sigma-Aldrich, Oakville, ON, Canada) culture media, supplemented with 10% fetal bovine serum (Life Technologies, Burlington, ON, Canada). HEY cells (obtained from Dr Ted Brown, Mount Sinai Hospital, Toronto, ON, USA) were maintained in RPMI-1640 (GE HyClone, Logan, UT, USA) medium containing 10% fetal bovine serum. Cells were regularly tested to be free of mycoplasma contamination.

Plasmids, transfection and RNA interference

FLAG-tagged cyclin G2 (FLAG-CCNG2) was generated and described previously.[7] All other plasmids were obtained from Addgene (Cambridge, MA, USA). To generate cell lines stably overexpressing cyclin G2, FLAG-CCNG2 was cloned into a viral vector, pBabe-puro.[43] Virus was produced by co-transfecting either pBabe-FLAG-CCNG2 or pBabe-empty vector, with a packaging plasmid, pUMVC and an envelope plasmid, pCMV-VSVg,[44] into 293T cells using the calcium phosphate protocol. Virus was harvested and used to infect each target cell line. Transient transfection of the FLAG-cyclin G2 or β-catenin-S33Y[45] was carried out using Lipofectamine 2000 (Life Technologies) according to the manufacturer's protocol. Lipofectamine RNAiMAX (Life Technologies) was used for the transfection of siRNAs targeting cyclin G2, E-cadherin or a non-targeting control (100 nM). The siRNAs (GenePharma Co, Shanghai, China) sequences are listed in Supplementary Table S1.

Oncomine data and tumor samples

Primary sources for the tumor data obtained from Oncomine (www.oncomine.org) were the following: Bonome,[46] Tothill,[47] Anglesio,[48] Yoshihara,[49] and Hendrix.[22] The sample size of each cohort is listed in the figure legend. Ovarian tumor samples were obtained from the Ottawa Ovarian Cancer Tissue Bank, through a protocol approved by the Research Ethics Board at The Ottawa Hospital, and with appropriate patient consent.

RNA extraction and qPCR

Total RNA from human ovary or Fallopian tube was purchased from Agilent Technologies (Mississauga, ON, Canada). Total RNA was extracted using TRIzol reagent (Life Technologies) following the manufacturer's protocol. RNA was reversed transcribed to cDNA using SuperScriptIII (Life Technologies). qPCR was carried out in 20 µl volumes containing 1 × EvaGreen qPCR master mix (Applied Biological Materials Inc., Richmond, BC, Canada) on the Qiagen Rotorgene Q (Valencia, CA, USA). Primers are listed in Supplementary Table S2. Glyceraldehyde-3-phosphate dehydrogenase (GAPDH) was used as an internal control. The relative expression levels of mRNA were quantified using the ΔΔCt method.

Western blotting analysis

Cells were lysed in a buffer containing 150 mM NaCl, 1% Nonidet P-40, 50 mM Tris/HCl (pH 7.4) supplemented with protease and phosphatase inhibitors (Life Technologies). Equal amounts of protein were separated by 10% sodium dodecyl sulfate–polyacrylamide gel electrophoresis and resolved by immunoblotting. Primary antibodies are listed in Supplementary Table S3. Proteins were visualized by Luminata Classico Western HRP Substrate (EMD Milipore, Etobicoke, ON, Canada). Where indicated, cells were treated with cyclohexamide (5 µg/ml, Sigma-Aldrich) prior to protein lysis. In some cases, cytoplasmic and nuclear fractions were separated using the NE-PER Extraction Kit (Life Technologies).

Immunofluorescence imaging and immunohistochemistry

Cells were fixed with 4% paraformaldehyde for 15 min, permeabilized with 0.2% Triton X-100 for 10 min, blocked with 1% bovine serum albumin for 30 min and incubated with anti-β-catenin-488 antibody (1:100), Palloidian–fluorescein isothiocyanate (50 µg/ml) or DYKDDDDK Tag-488 antibody (FLAG detection, 1:100) in phosphate-buffered saline containing 1% bovine serum albumin and 4,6-diamidino-2-phenylindole (1 µg/ml) for nuclear imaging. Microscopy was performed using a Zeiss LSM 700 confocal microscope (Toronto, ON, Canada).

Immunohistochemistry of mouse tumors was performed as described previously.[50] Some sections were stained with hematoxylin and eosin and others employed anti-E-cadherin as a primary antibody. Biotinylated secondary antibody was followed by conjugated horseradish peroxidase provided by the Vectastain ABC Kit (PK-4000, Vector Laboratories, Burlington, ON, Canada). The slides were then counterstained with 3,3′ diaminobenzidine and Mayer's Hematoxylin.

Cell growth, proliferation and clonogenic assays

Cells were seeded at a density of 50 000 cells per well in a six-well plate and maintained in media containing 10% fetal bovine serum. At the end of the experiment, cell number was determined using trypan blue exclusion. Cell proliferation assays were carried out using the bromodeoxyuridine (BrdU) cell proliferation assay kit (BioVision, Milpitas, CA, USA) according to the manufacturer's protocol. Briefly, 10 000 cells/well were seeded into a 96-well plate and incubated for 72 h prior to addition of the BrdU solution. BrdU incorporation was measured by absorbance at 450 nm. For clonogenic assay, cells were seeded onto 60 mm culture dishes at the density of 1000 cells/well. Cultures were maintained for 9–12 days in complete culture media until colonies appeared. The colonies were fixed with 4% paraformaldehyde and stained with 0.5% crystal violet. The plates were photographed and the numbers of visible colonies were counted.

Migration and invasion assays

Cell migration was determined using wound healing and transwell migration assays as previously reported.[51] Cells were photographed by a Nikon Eclipse TE2000-U fluorescence microscope (Mississauga, ON, Canada) at × 100 total magnification and counted using Image J (NIH, Bethesda, MD, USA). Transwell invasion assays were performed in the same manner as the transwell migration assay with the exception that transwell inserts were precoated with growth-factor-reduced Matrigel (1:40, BD Biosciences, Mississauga, ON, Canada). In some experiments, cells were treated with a proliferation inhibitor, mitomycin C (10 µg/ml, Sigma-Aldrich) for 2 h prior to the migration/invasion assay.

Spheroid formation and 3D migration assay

A hanging drop culture[21] was used to determine the ability of cells to form spheroids. Briefly, at least 20 droplets containing 20 000 cells in 20 µl were plated into the inner surface of Petri dish cover. The covers were inverted and placed on a dish containing 15 ml of phosphate-buffered saline. Spheroids were photographed on the fourth day after plating. For 3D migration assays, spheroids were embedded into two layers of rat-tail collagen I (BD Biosciences) in a 96-well plate. Images were recorded immediately after polymerization, 3 and 6 days later. Cell migration was visualized by cellular penetration into the surrounding matrix.

TOPFlash reporter assay

TOPflash reporters assay was used for the detection of β-catenin/TCF transcriptional activity. Cells were transiently co-transfected with TOPflash reporter construct and Renilla control plasmid. The Dual-Luciferase Reporter Assay System (Promega, Fitchburg, WI, USA) was used to detect the activities of Firefly and Renilla according to the manufacturer's protocol.

Tumor-formation assays

All animal protocols received institutional animal care committee approval for animal research, and work was conducted in accordance to the guidelines of the Canadian Council on Animal Care. Female 4–6-week-old CD1 nude mice (Charles River Laboratories, St-Constant, QC, Canada) were randomized into two groups for *in vivo* tumor studies. In all, 1×10^6 cells were used for subcutaneous and 5×10^6 cells were used for intraperitoneal injection. Mice were killed and photographed. Tumors were excised, weighed and measured for subcutaneous injection, and total body weight was recorded for intraperitoneal injection. Investigators were not blinded for animal studies. For subcutaneous injection, one mouse from the control group was excluded based on unusual tumor regression after day 43. Group size was selected based on experience with xenograft models and in compliance with the guideline of the animal care committee to use the minimum number of animals required. The number of mice used in each experiment is indicated in figure legends.

Statistical analyses

Results are expressed as mean ± s.e.m. from a representative experiment, and the number of replicates is indicated in figure legends. Each experiment was repeated two to three times. Group size was selected based on cell and reagent limitations while still achieving statistically relevant results. One-way analysis of variance was used to determine the difference among multiple groups, followed by Newman–Keul's test. Comparison of two groups was performed by two-sided Student's *t*-test. F-tests were used to determine the variance between each group, and normal distribution was assessed by D'Agostino–Pearson test for normality (n values >8). GraphPad Prism (La Jolla, CA, USA) was used to conduct statistical testing, and significance was defined as $P < 0.05$.

CONFLICT OF INTEREST

The authors declare no conflict of interest.

ACKNOWLEDGEMENTS

This study was supported by grants from Canadian Institutes of Health Research (CIHR) to CP (MOP-89931) and from Natural Science and Engineering Foundation (NSERC) to CP (203081-2009) and to BY (227937-2012). SB was a recipient of graduate scholarships from NSERC, OGS and York University. We thank Dr Mien-Chie Hung for SKOV3.ip1 cells and the tumor bank at Ottawa Hospital Research Institute for providing the ovarian cancer samples. The Ottawa Ovarian Cancer Tissue Bank is supported in part by Ovarian Cancer Canada.

REFERENCES

1 Ye G, Bernaudo S, Peng C. Etiology and overview. In: Schwartz PE (ed), *Advances in Ovarian Cancer Management*. Future Medicine Ltd: London, UK, 2012, pp 6–16.
2 Bell D, Berchuck A, Birrer M, Chien J, Cramer DW, Dao F *et al.* Integrated genomic analyses of ovarian carcinoma. *Nature* 2011; **474**: 609–615.
3 Horne MC, Goolsby GL, Donaldson KL, Tran D, Neubauer M, Wahl AF. Cyclin G1 and cyclin G2 comprise a new family of cyclins with contrasting tissue-specific and cell cycle-regulated expression. *J Biol Chem* 1996; **271**: 6050–6061.
4 Horne MC, Donaldson KL, Goolsby GL, Tran D, Mulheisen M, Hell JW *et al.* Cyclin G2 is up-regulated during growth inhibition and B cell antigen receptor-mediated cell cycle arrest. *J Biol Chem* 1997; **272**: 12650–12661.
5 Kasukabe T, Okabe-Kado J, Kato N, Sassa T, Honma Y. Effects of combined treatment with rapamycin and cotylenin A, a novel differentiation-inducing agent, on human breast carcinoma MCF-7 cells and xenografts. *Breast Cancer Res* 2005; **7**: R1097–R1110.
6 Gajate C, An F, Mollinedo F. Differential cytostatic and apoptotic effects of ecteinascidin-743 in cancer cells. Transcription-dependent cell cycle arrest and transcription-independent JNK and mitochondrial mediated apoptosis. *J Biol Chem* 2002; **277**: 41580–41589.
7 Xu G, Bernaudo S, Fu G, Lee DY, Yang BB, Peng C. Cyclin G2 is degraded through the ubiquitin-proteasome pathway and mediates the antiproliferative effect of activin receptor-like kinase 7. *Mol Biol Cell* 2008; **19**: 4968–4979.
8 Bennin DA, Don AS, Brake T, McKenzie JL, Rosenbaum H, Ortiz L *et al.* Cyclin G2 associates with protein phosphatase 2A catalytic and regulatory B′ subunits in active complexes and induces nuclear aberrations and a G1/S phase cell cycle arrest. *J Biol Chem* 2002; **277**: 27449–27467.
9 Liu J, Cui ZS, Luo Y, Jiang L, Man XH, Zhang X. Effect of cyclin G2 on proliferative ability of SGC-7901 cell. *World J Gastroenterol* 2004; **10**: 1357–1360.
10 Kim Y, Shintani S, Kohno Y, Zhang R, Wong DT. Cyclin G2 dysregulation in human oral cancer. *Cancer Res* 2004; **64**: 8980–8986.
11 Choi MG, Noh JH, An JY, Hong SK, Park SB, Baik YH *et al.* Expression levels of cyclin G2, but not cyclin E, correlate with gastric cancer progression. *J Surg Res* 2009; **157**: 168–174.
12 Adorno M, Cordenonsi M, Montagner M, Dupont S, Wong C, Hann B *et al.* A Mutant-p53/Smad complex opposes p63 to empower TGFbeta-induced metastasis. *Cell* 2009; **137**: 87–98.
13 Kalluri R, Weinberg RA. The basics of epithelial-mesenchymal transition. *J Clin Invest* 2009; **119**: 1420–1428.
14 Burleson KM, Hansen LK, Skubitz AP. Ovarian carcinoma spheroids disaggregate on type I collagen and invade live human mesothelial cell monolayers. *Clin Exp Metastasis* 2004; **21**: 685–697.
15 Pease JC, Brewer M, Tirnauer JS. Spontaneous spheroid budding from monolayers: a potential contribution to ovarian cancer dissemination. *Biol Open* 2012; **1**: 622–628.
16 Arend RC, Londono-Joshi AI, Straughn Jr JM, Buchsbaum DJ. The Wnt/beta-catenin pathway in ovarian cancer: a review. *Gynecol Oncol* 2013; **131**: 772–779.
17 Clevers H, Nusse R. Wnt/beta-catenin signaling and disease. *Cell* 2012; **149**: 1192–1205.
18 Yook JI, Li XY, Ota I, Hu C, Kim HS, Kim NH *et al.* A Wnt-Axin2-GSK3beta cascade regulates Snail1 activity in breast cancer cells. *Nat Cell Biol* 2006; **8**: 1398–1406.
19 Zhu LY, Zhang WM, Yang XM, Cui L, Li J, Zhang YL *et al.* Silencing of MICAL-L2 suppresses malignancy of ovarian cancer by inducing mesenchymal-epithelial transition. *Cancer Lett* 2015; **363**: 71–82.
20 Fu G, Peng C. Nodal enhances the activity of FoxO3a and its synergistic interaction with Smads to regulate cyclin G2 transcription in ovarian cancer cells. *Oncogene* 2011; **30**: 3953–3966.
21 Sodek KL, Ringuette MJ, Brown TJ. Compact spheroid formation by ovarian cancer cells is associated with contractile behavior and an invasive phenotype. *Int J Cancer* 2009; **124**: 2060–2070.
22 Hendrix ND, Wu R, Kuick R, Schwartz DR, Fearon ER, Cho KR. Fibroblast growth factor 9 has oncogenic activity and is a downstream target of Wnt signaling in ovarian endometrioid adenocarcinomas. *Cancer Res* 2006; **66**: 1354–1362.
23 Shell S, Park SM, Radjabi AR, Schickel R, Kistner EO, Jewell DA *et al.* Let-7 expression defines two differentiation stages of cancer. *Proc Natl Acad Sci USA* 2007; **104**: 11400–11405.
24 Lau MT, Klausen C, Leung PC. E-cadherin inhibits tumor cell growth by suppressing PI3K/Akt signaling via beta-catenin-Egr1-mediated PTEN expression. *Oncogene* 2011; **30**: 2753–2766.
25 ten Berge D, Koole W, Fuerer C, Fish M, Eroglu E, Nusse R. Wnt signaling mediates self-organization and axis formation in embryoid bodies. *Cell Stem Cell* 2008; **3**: 508–518.
26 Conacci-Sorrell M, Simcha I, Ben-Yedidia T, Blechman J, Savagner P, Ben-Ze'ev A. Autoregulation of E-cadherin expression by cadherin-cadherin interactions: the roles of beta-catenin signaling, Slug, and MAPK. *J Cell Biol* 2003; **163**: 847–857.
27 Ito Y, Yoshida H, Uruno T, Nakano K, Takamura Y, Miya A *et al.* Decreased expression of cyclin G2 is significantly linked to the malignant transformation of papillary carcinoma of the thyroid. *Anticancer Res* 2003; **23**: 2335–2338.
28 Jia JS, Xu SR, Ma J, Ha S, Guo XN, Wang Y. [Expression of cyclin g2 mRNA in patients with acute leukemia and its clinical significance]. *J Exp Hematol* 2005; **13**: 254–259.
29 Martinez-Gac L, Marques M, Garcia Z, Campanero MR, Carrera AC. Control of cyclin G2 mRNA expression by forkhead transcription factors: novel mechanism for cell cycle control by phosphoinositide 3-kinase and forkhead. *Mol Cell Biol* 2004; **24**: 2181–2189.
30 Davidowitz RA, Selfors LM, Iwanicki MP, Elias KM, Karst A, Piao H *et al.* Mesenchymal gene program-expressing ovarian cancer spheroids exhibit enhanced mesothelial clearance. *J Clin Invest* 2014; **124**: 2611–2625.
31 Lili LN, Matyunina LV, Walker LD, Wells SL, Benigno BB, McDonald JF. Molecular profiling supports the role of epithelial-to-mesenchymal transition (EMT) in ovarian cancer metastasis. *J Ovarian Res* 2013; **6**: 49.
32 Chiu WT, Huang YF, Tsai HY, Chen CC, Chang CH, Huang SC *et al.* FOXM1 confers to epithelial-mesenchymal transition, stemness and chemoresistance in epithelial ovarian carcinoma cells. *Oncotarget* 2015; **6**: 2349–2365.
33 Ponnusamy MP, Lakshmanan I, Jain M, Das S, Chakraborty S, Dey P *et al.* MUC4 mucin-induced epithelial to mesenchymal transition: a novel mechanism for metastasis of human ovarian cancer cells. *Oncogene* 2010; **29**: 5741–5754.
34 Yuan H, Kajiyama H, Ito S, Yoshikawa N, Hyodo T, Asano E *et al.* ALX1 induces snail expression to promote epithelial-to-mesenchymal transition and invasion of ovarian cancer cells. *Cancer Res* 2013; **73**: 1581–1590.
35 Haynes J, Srivastava J, Madson N, Wittmann T, Barber DL. Dynamic actin remodeling during epithelial-mesenchymal transition depends on increased moesin expression. *Mol Biol Cell* 2011; **22**: 4750–4764.
36 Lamouille S, Xu J, Derynck R. Molecular mechanisms of epithelial-mesenchymal transition. *Nat Rev Mol Cell Biol* 2014; **15**: 178–196.
37 Gonzalez DM, Medici D. Signaling mechanisms of the epithelial-mesenchymal transition. *Sci Signal* 2014; **7**: re8.
38 Ford CE, Jary E, Ma SS, Nixdorf S, Heinzelmann-Schwarz VA, Ward RL. The Wnt gatekeeper SFRP4 modulates EMT, cell migration and downstream Wnt signalling in serous ovarian cancer cells. *PLoS One* 2013; **8**: e54362.
39 Aguilar V, Annicotte JS, Escote X, Vendrell J, Langin D, Fajas L. Cyclin G2 regulates adipogenesis through PPAR gamma coactivation. *Endocrinology* 2010; **151**: 5247–5254.
40 Mourgues L, Imbert V, Nebout M, Colosetti P, Neffati Z, Lagadec P *et al.* The BMI1 polycomb protein represses cyclin G2-induced autophagy to support proliferation in chronic myeloid leukemia cells. *Leukemia* 2015; **10**: 1993–2002.
41 Gao C, Cao W, Bao L, Zuo W, Xie G, Cai T *et al.* Autophagy negatively regulates Wnt signalling by promoting Dishevelled degradation. *Nat Cell Biol* 2010; **12**: 781–790.

42 Stamos JL, Weis WI. The beta-catenin destruction complex. *Cold Spring Harb Perspect Biol* 2013; **5**: a007898.
43 Morgenstern JP, Land H. Advanced mammalian gene transfer: high titre retroviral vectors with multiple drug selection markers and a complementary helper-free packaging cell line. *Nucleic Acids Res* 1990; **18**: 3587–3596.
44 Stewart SA, Dykxhoorn DM, Palliser D, Mizuno H, Yu EY, An DS *et al.* Lentivirus delivered stable gene silencing by RNAi in primary cells. *RNA* 2003; **9**: 493–501.
45 Kolligs FT, Hu G, Dang CV, Fearon ER. Neoplastic transformation of RK3E by mutant beta-catenin requires deregulation of Tcf/Lef transcription but not activation of c-myc expression. *Mol Cell Biol* 1999; **19**: 5696–5706.
46 Bonome T, Levine DA, Shih J, Randonovich M, Pise-Masison CA, Bogomolniy F *et al.* A gene signature predicting for survival in suboptimally debulked patients with ovarian cancer. *Cancer Res* 2008; **68**: 5478–5486.
47 Tothill RW, Tinker AV, George J, Brown R, Fox SB, Lade S *et al.* Novel molecular subtypes of serous and endometrioid ovarian cancer linked to clinical outcome. *Clin Cancer Res* 2008; **14**: 5198–5208.
48 Anglesio MS, Arnold JM, George J, Tinker AV, Tothill R, Waddell N *et al.* Mutation of ERBB2 provides a novel alternative mechanism for the ubiquitous activation of RAS-MAPK in ovarian serous low malignant potential tumors. *Mol Cancer Res* 2008; **6**: 1678–1690.
49 Yoshihara K, Tajima A, Komata D, Yamamoto T, Kodama S, Fujiwara H *et al.* Gene expression profiling of advanced-stage serous ovarian cancers distinguishes novel subclasses and implicates ZEB2 in tumor progression and prognosis. *Cancer Sci* 2009; **100**: 1421–1428.
50 Siragam V, Rutnam ZJ, Yang W, Fang L, Luo L, Yang X *et al.* MicroRNA miR-98 inhibits tumor angiogenesis and invasion by targeting activin receptor-like kinase-4 and matrix metalloproteinase-11. *Oncotarget* 2012; **3**: 1370–1385.
51 Nadeem L, Munir S, Fu G, Dunk C, Baczyk D, Caniggia I *et al.* Nodal signals through activin receptor-like kinase 7 to inhibit trophoblast migration and invasion: implication in the pathogenesis of preeclampsia. *Am J Pathol* 2011; **178**: 1177–1189.

Supplementary Information accompanies this paper on the Oncogene website (http://www.nature.com/onc)